Modelling hydrological responses of the Athabasca River basin to climate change by the Modified ISBA Land Surface Scheme

ERNST KERKHOVEN & THIAN YEW GAN

*Markin/CNRL NREF 3-033, Department of Civil and Environmental Engineering,
University of Alberta, Edmonton, Alberta T6G 2W2, Canada*

tgan@ualberta.ca

Abstract The major climate input data to ISBA (Interactions Soil–Biosphere–Atmosphere) for hydrological modelling of the Athabasca River basin (ARB) are the archived forecasts from the Global Environmental Multiscale Model (GEM), and ERA-40 data of ECMWF. We modified the sub-grid runoff algorithm of ISBA by assuming that the sub-grid distribution of soil moisture follows the Xinanjiang distribution. Simulations by the modified ISBA using the mesoscale resolution GEM data and the GCM-scale ERA-40 re-analysis data showed that these modifications significantly improved model performance, and for the latter data set, it was possible to reproduce the observed streamflow in Athabasca without using downscaling methods. However, a simple statistical downscaling algorithm based on the high resolution GEM data on ERA-40 data further improved the simulated streamflow of ARB. The predicted changes to mean monthly temperature and precipitation from seven GCMs for four SRES climate scenarios over the 1961–1990 base period were used to adjust the ERA-40 temperature and precipitation for ARB, over three 30-year time periods (2010–2039, 2040–2069, 2070–2100) (a total of 54 simulations). Most of the models predict continuing decreases in average, maximum, and minimum flows over the next 100 years.

Key words Athabasca River basin; hydrological response modelling;
ISBA (Interactions Soil–Biosphere–Atmosphere) ; streamflow prediction;
streamflow simulation

INTRODUCTION

As an overall strategy of the Canadian GEWEX programme (MAGS2) to develop basin-scale representations of water and energy cycles of the Mackenzie River Basins (MRB) through atmosphere–surface hydrological modelling, large-scale observations and data assimilation techniques, we modified the land surface scheme, ISBA (Interactions Soil–Biosphere–Atmosphere) of Météo France (Noilhan & Planton, 1989), to the Athabasca River basin (ARB) below Fort McMurray (Fig. 1) to assess potential changes to its hydrological responses between historical and climate change scenarios. We used observed data and data supplied by atmospheric models to simulate the interaction between the atmosphere and ARB, in which interflow due to muskeg plays an important component in the sub-surface runoff. The local runoff predicted by the modified ISBA was then used as input for a hydrological routing model to simulate the total streamflow at the basin outlet.
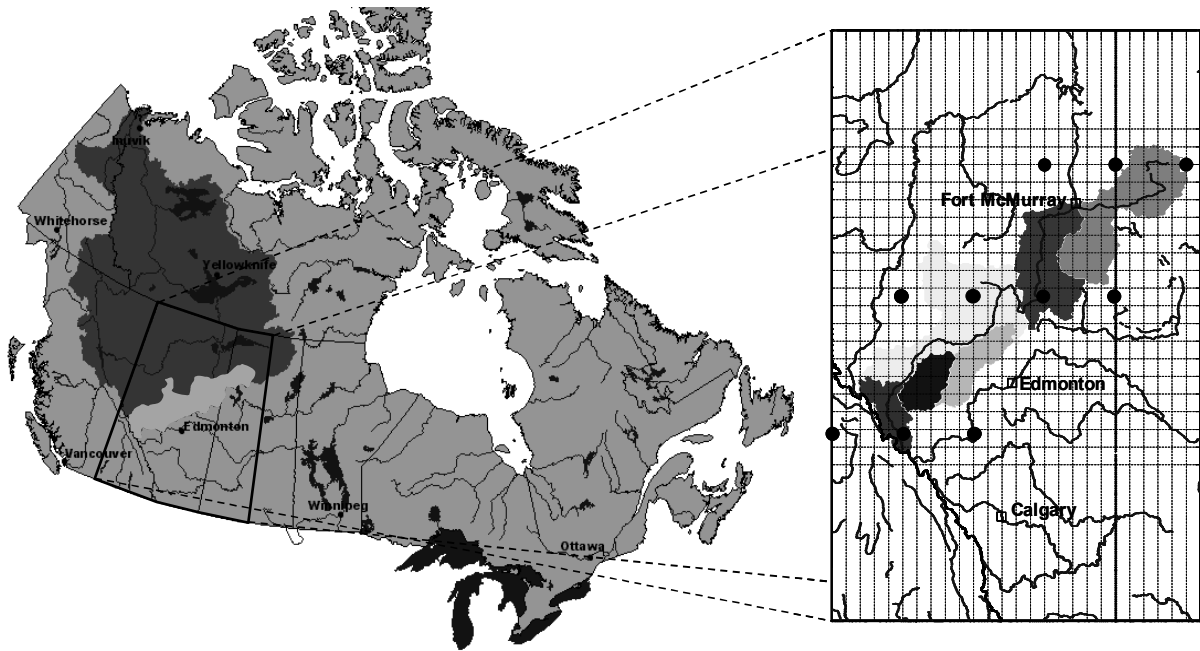
Fig. 1 DEM derived extent of the Athabasca River below Fort McMurray Basin with GEM grid (dashed lines) and ERA-40 grid (solid circles) overlaid.

METHODOLOGY AND DATA

Two sources of meteorological data were used. The first is a set of archived forecasts from the Meteorological Survey of Canada's Global Environmental Multiscale Model (GEM), and the second is the ERA-40 historical re-analysis data developed by the European Centre for Mid-range Weather Forecasts (ECMWF). The GEM archive covers western Canada from October 1995 to September 2001 while ERA-40 has global coverage from January 1961 to August 2002. The GEM data have a spatial resolution of 0.33° latitude and 0.50° longitude and a temporal resolution of 3 hours. The ERA-40 data have a spatial resolution of 2.5° latitude and 2.5° longitude and a temporal resolution of 6 hours.

ISBA, designed to model land surface physics that control the energy and water budgets, has parameters divided into two categories: four primary parameters that are specified at each grid point (% sand, % clay, vegetation type, and land–water ratio), and 22 secondary parameters, which are determined from the primary parameters. The Ecoclimap land-use data set (Masson *et al.*, 2003), which includes all the physical parameters needed to run ISBA, was used to define the surface parameters of ISBA. Ecoclimap covers the entire globe with a horizontal resolution of 30 arc-seconds (approx. 1 km) and was derived by combining existing land-cover and climate maps, in addition to using the AVHRR satellite data. Basin characteristics, such as areal extent and the drainage network, were derived from the 6 arc-second (approximately 200-m resolution) digital elevation model (DEM) of the Peace-Athabasca River basin. To facilitate cross-referencing across the data sets, each DEM square was linked to its nearest land-use data square, and each land-use data square was linked to its nearest meteorological grid square.

Representing the land cover as a mosaic of tiles and adjusting the meteorological data for each tile's mean elevation can account for a large part of the spatial heterogeneity of land cover and topography. This accounting is primarily limited by the variation in topography within each land cover tile. The 6 arc-second (200 m) resolution was also used to determine the extent and flow network of the ARB. With the flow directions determined, the basin extent was determined by finding all the squares in the DEM that drained to the outlet. The area of ARB below Fort McMurray was about 133 606 km^2 with a main channel length of 1119 km. Channel routing was performed using the Ponce & Yevjevich (1978) variation of the Muskingum-Cunge scheme (Cunge, 1969), a kinematic routing scheme that approximates a diffusive wave by equating the numerical diffusion of the scheme with the physical diffusion. This scheme was applied to each of the hydrological grid squares in the basin starting with the farthest upstream, and ending at the basin outlet. Channel reach lengths are on the order of 2000 m and all channel cross-sections are assumed to be rectangular in shape, which include channel characteristics for 21 reaches in the Athabasca River basin.

MODIFICATION TO ISBA's RUNOFF SCHEME WITH SUB-GRID HETEROGENEITY

Habets *et al.* (1999) developed a sub-grid runoff scheme that statistically considers the sub-grid heterogeneity of soil moisture, *x*, to follow the Xinanjiang distribution:

$$F(x) = 1 - \left(1 - \frac{x}{x_{max}}\right)^\beta \qquad 0 \leq x \leq x_{max} \tag{1}$$

$$\frac{\bar{x}}{x_{max}} = \frac{1}{\beta + 1} \tag{2}$$

where β is an empirical parameter, and $F(x)$ is the cumulative probability distribution of *x*, defined by the maximum (x_{max}) and mean values of *x*, $\bar{x}$. When the modeller sets β they are effectively defining the maximum bucket size (or soil depth) in the grid. A gravity drainage scheme was developed to represent sub-surface runoff:

$$Q = C_3(w - w_{drain})D \tag{3}$$

where Q is the sub-surface runoff, D is the depth of the deep soil layer, w is the soil water content, w_{drain} is the minimum soil water content where drainage will occur, and C_3 is a coefficient. ISBA therefore treats sub-surface runoff as a linear reservoir. ISBA requires two parameters: β, and the minimum soil water content for drainage, both of which require calibration which can become problematic when applied to large river basins where they could vary widely. To eliminate this difficulty, these two parameters were removed by making them functions of the soil characteristics. First, runoff was made a function of soil water retention:

$$S = \left(\frac{w - w_r}{w_{sat} - w_r}\right) \tag{4}$$

where S is the soil water retention, w_r is the residual water content, and w_{sat} is the saturated water content. Because the maximum possible retention is 1, and since the model predicts the average water retention at each time step, β can be derived from equation (2) for each time step as:

$$\beta = \frac{1}{\overline{\overline{S}}} - 1 \tag{5}$$

Assuming rainfall follows an exponential distribution (Entekhabi & Eagleson, 1989), it can then be shown that S_r, the surface runoff at an area where S exceeds 1, is given by:

$$S_r = \frac{\Delta S^{\beta+1}}{\beta+1}\frac{\gamma(\beta+2, k/\Delta S)}{k^\beta} + \exp\left(-\frac{k}{\Delta S}\right)\left[\Delta S + \frac{k}{\beta+1}\right] \tag{6}$$

where ΔS is the additional soil water retention due to rainfall, k is the fraction of the total area that receives rainfall and $\gamma(a,b)$ is Euler's lower incomplete gamma function.

This method eliminates β as a user defined parameter. The other parameter was eliminated by assuming that w_{drain} equals w_r, which can be calculated from the soil texture using, say, the Brooks-Corey equation for hydraulic conductivity of unsaturated soils. Equation (3) was altered into a function of soil water retention:

$$Q = C_3\left(\frac{w - w_r}{w_{sat} - w_r}\right)^{3+\frac{2}{\lambda}} D = C_3 D S^{3+\frac{2}{\lambda}} \tag{7}$$

where λ is the Brooks-Corey pore-size index which can also be calculated from the soil texture using a pedo-transfer function. If we assume that the sub-grid distribution of soil moisture follows the Xinanjiang distribution, the total sub-surface runoff produced is:

$$Q = \int_0^1 Q(S)f(S)\mathrm{d}S \tag{8}$$

where $f(S) = \beta(1 - S)^{\beta-1}$ (by differentiating equation (1)). The integration of equation (8) is similar in form to the Euler's beta function, from which it can be shown that:

$$Q = C_3 D \frac{\Gamma(n+1)\Gamma(\beta+1)}{\Gamma(n+\beta+1)} \tag{9}$$

where $\Gamma(x)$ is Euler's gamma function, and $\Gamma(x) = (x - 1)!$ when x is an integer. This equation is highly nonlinear and produces much lower runoff rates under dry conditions than the original ISBA scheme. Under moist conditions, when β approaches 0 the two methods will predict similar runoff rates.

DISCUSSIONS OF RESULTS

The GEM meteorological data were divided into a calibration period (October 1996–June 1998) and a verification period (July 1998–September 2001). The calibration
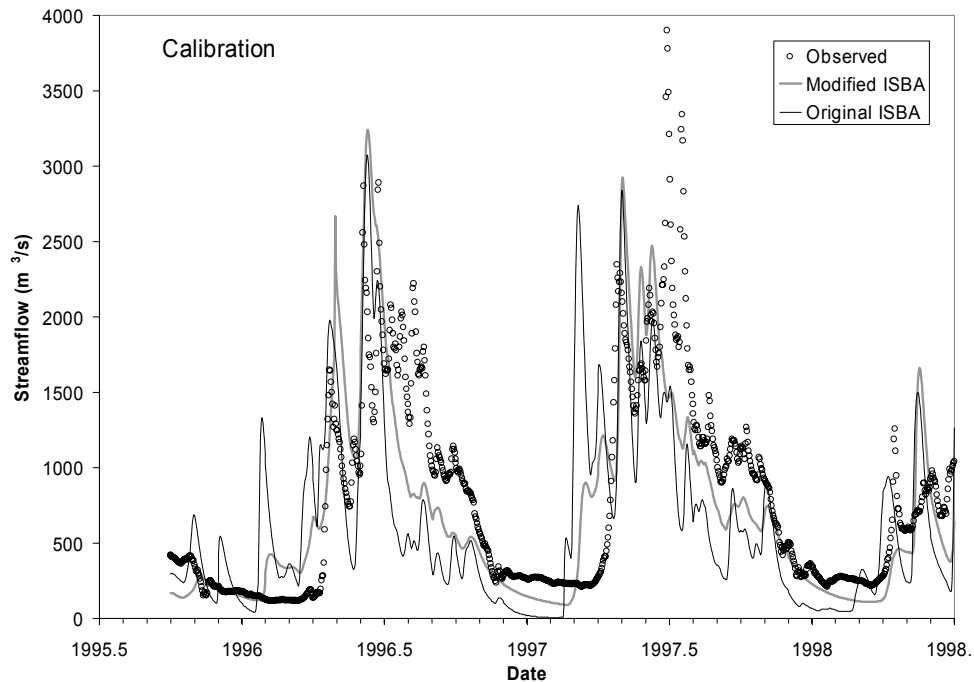
Fig. 2 ISBA/GEM calibration (1995–1998) hydrographs.

Table 1 Summary statistics of calibration and validation errors of MISBA.

		R^2	Absolute error	RMSE	Log error
GEM	Cab	0.59	0.40	0.576	0.078
	Val	0.77	0.26	0.44	0.05
ERA-40	Cab	0.62	0.36	0.64	0.06
	Val	0.57	0.38	0.63	0.06
ERA-40/GEM	Cab	0.77	0.29	0.50	0.05
	Val	0.68	0.31	0.52	0.05

and verification runs were both initialized on 1 October 1995. One set of calibration and verification runs were made using the Modified ISBA scheme (MISBA) briefly described above. Figure 2 shows the calibration hydrographs for MISBA, which matches the observed streamflow reasonably well because it uses a nonlinear approach (equation (7)), as against the linear approach of the original ISBA (OISBA), which produced much poorer match with the observed hydrograph (see Kerkhoven & Gan, 2004, for details). This nonlinear approach results in a longer retention time and a more realistic recession curve. Besides, the soil rarely becomes moist enough to produce any noticeable surface runoff. MISBA, although dominated by sub-surface runoff, does predict some surface runoff during periods of rapid snowmelt and intense precipitation and this runoff was found to improve MISBA's performance.

Comparing the error statistics in Table 1 for the GEM and ERA-40 simulations during the overlap period (October 1995–September 2001) reveals similar overall skill with the ERA-40 simulations generally performing better during the GEM calibration period and worse during the verification period. Unlike the GEM simulations, there is no significant improvement in performance between the GEM calibration and GEM

verification periods in the ERA-40 simulations and therefore Table 1 only shows the error statistics for the full overlap period.

At 2.5° × 2.5°, ERA-40 data is of GCM resolution, and so downscaling the data could potentially improve the simulation of ARB's streamflow. Only a simple, parsimonious statistical downscaling scheme is considered here. Given that the GEM archive is of much higher resolution than ERA-40 data, we can directly compare the mean monthly meteorological GEM data for each grid point with the mean monthly meteorological data for the nearest ERA-40 grid point during the period that the two data sets overlap (October 1995–September 2001). Downscaling was achieved by simply shifting the ERA-40 data to match the monthly mean of each GEM point. For example, if the January precipitation of a GEM point was 10% higher than its closest ERA-40 point during the overlap period, all the January ERA-40 precipitation rates for this point were increased by 10%. Radiation, humidity, air pressure, and wind speed data were handled in the same way while temperature was simply shifted by the difference in mean temperature.

This algorithm does not address limitations of ERA-40's temporal scales and spatial variability and therefore should not improve the simulation of summer storms. However, it will better represent the spatial distribution of land cover, topography, and local climate and should therefore improve the simulation of snowmelt and evaporation. Comparing the error statistics in Table 1 for the GEM and ERA-40/GEM simulations during the overlap period shows that the ERA-40/GEM simulations are just as accurate as the GEM simulations. This suggests that this simple algorithm accounts for the majority of the heterogeneity between the ERA-40 and GEM scales. Comparing the error statistics for the ERA-40 and ERA-40/GEM simulations shows that the ERA-40/GEM simulations are superior by every error measure.

Figure 3 is a plot of the full hydrograph from January 1961 to August 2002 for the ERA-40/GEM hydrographs where the most noticeable improvement in the MISBA hydrograph is the reduction of a number of anomalous peaks in the MISBA/ERA-40 hydrograph (not shown) without compromising the non-anomalous peaks.

For 40 years of ERA-40/GEM simulations, the mean and variance of simulated values were compared with the observed data by the classic t test and the F test. MISBA passed the t test 287 days of the year and the F test 242 days of the year. Again, the MISBA/ERA-40/GEM simulation is the best of all the simulations in this study while the old ISBA/ERA-40 simulation (not shown) is the poorest.

POSSIBLE IMPACTS OF CLIMATE CHANGE TO ATHABASCA RIVER BASIN

MISBA/ERA-40 was used to simulate a number of SRES climate scenarios for the Athabasca River basin. The predicted changes to mean monthly temperature and precipitation from seven GCM models (CCSRNIES, CGCM2, CSIROMk2b, ECHAM4, GFDLR30, HadCM3, and NCARPCM) for four SRES climate scenarios (A1FI, A21, B11, B21) (Fig. 4) over the 1961–1990 base period were used to adjust the ERA-40 temperature and precipitation for ARB, over three 30-year time periods: 2010–2039 (early 21st century), 2040–2069 (mid 21st century), and 2070–2099 (late
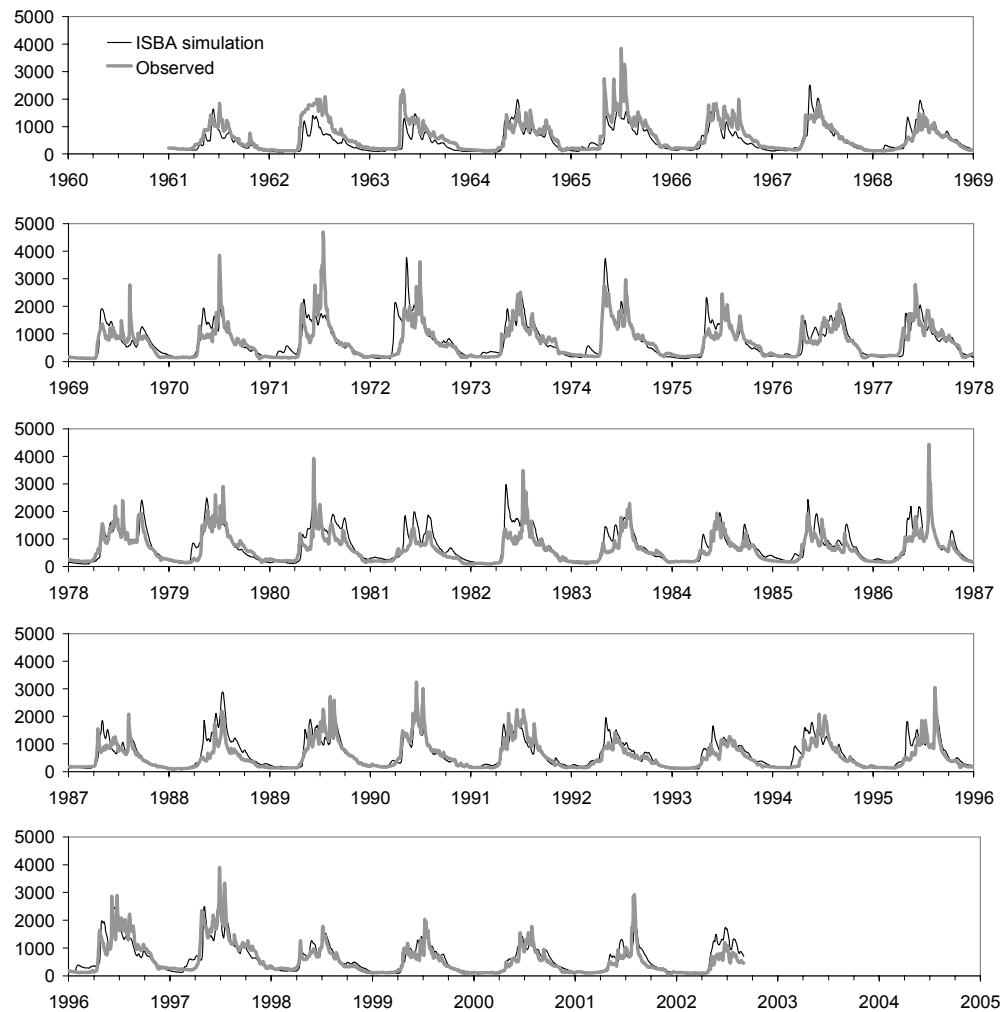
Fig. 3 Observed and MISBA/ERA-40/GEM simulation hydrographs.

21st century). Only two GCMs simulated all four scenarios (HadCM3 and CCRNIES). The other five GCMS only simulated the A2 and B2 scenarios. A total of 18 future climates scenarios were run for each 30-year period (two A1F1 predictions, seven A21 predictions, two B11 predictions, and seven B21 predictions) for a total of 54 simulations.

In general, the predictions were more sensitive to the model used than the scenario selected. However, most of the models predict continuing decreases in average, maximum, and minimum flows over the next 100 years. A summary of the GCM predictions for annual temperature and precipitation changes in the ARB is shown in Fig. 4. The colour of the dot indicates the time period while the surrounding shape indicates the GCM. In general, the GCMs predict an increase in both temperature and precipitation. HadCM3 is the wettest, ECHAM4 is the driest, and CCSRNIES is the warmest. CGCM2's predictions fall in the middle.

Changes in predicted runoff are weakly correlated with precipitation changes. All 18 GCM scenarios predict decreased streamflow by the end of the 21st century. Two thirds of the scenarios predict stream flows to decline by over 20% (Fig. 5). On the
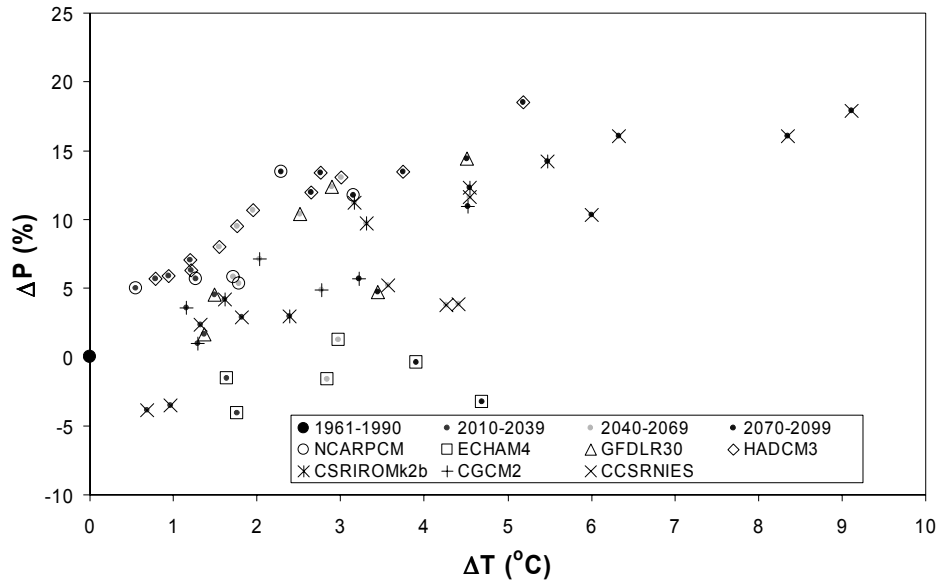
Fig. 4 Precipitation and temperature changes in the Athabasca River basin predicted by SRES climate scenarios.
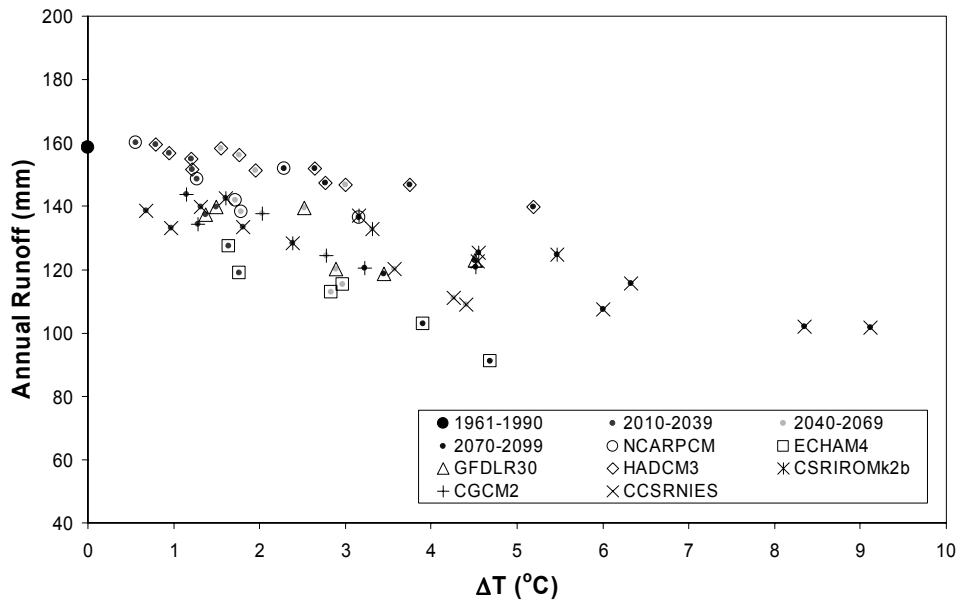

Fig. 5 Mean annual runoff and change in temperature.

other hand, the runoff coefficient is very strongly correlated with changes in temperature. In general, for every degree temperature rises the runoff coefficient drops by 8% (Fig. 6).

As can be seen in Fig. 7, the size of the mean annual snow pack in the basin is strongly co-related with mean annual flow in the basin. With the exception of the HadCM3 GCM (which is by far the wettest in December and January) the scenarios
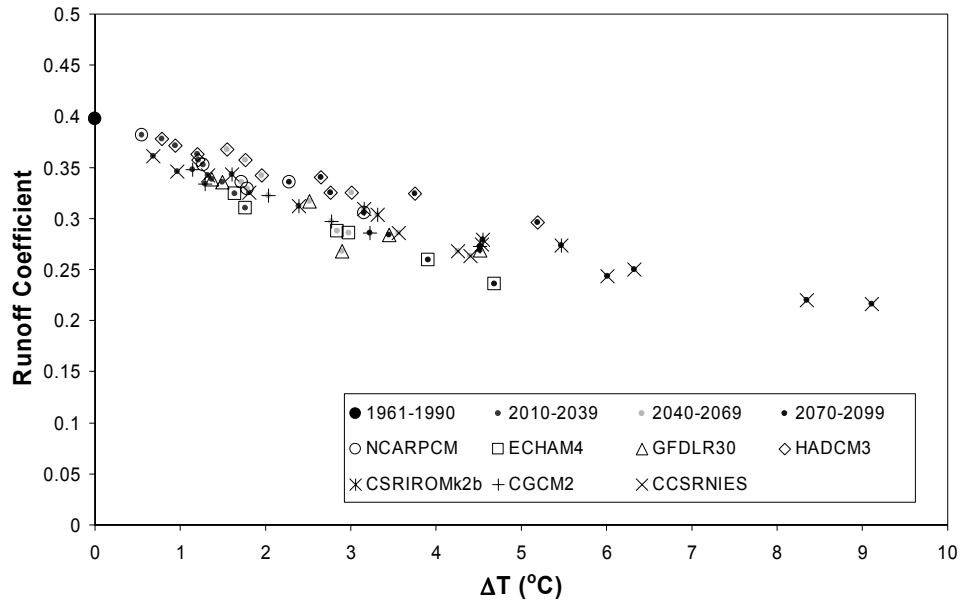
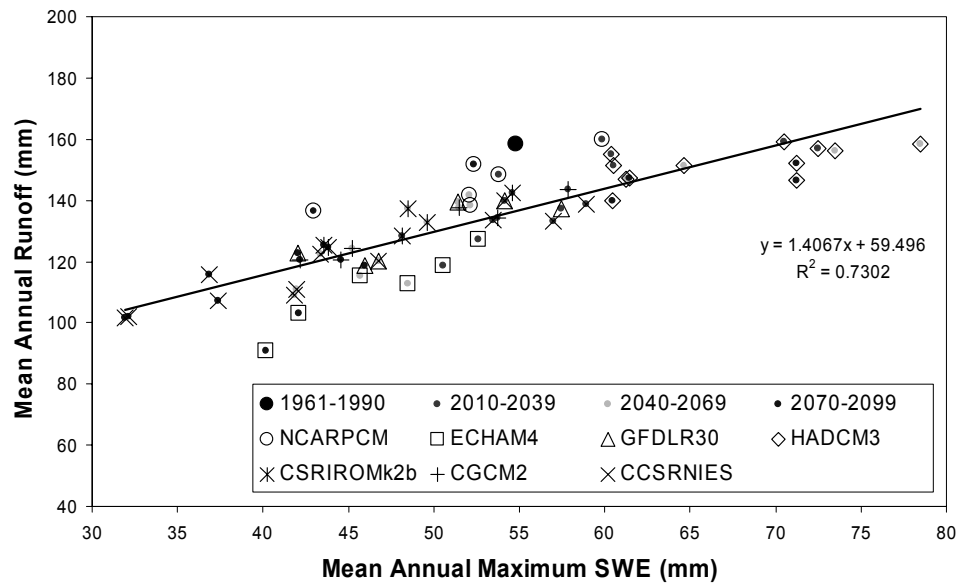**Fig. 6** Changes of runoff coefficient with changes in temperature.

Fig. 7 Mean annual runoff *vs* mean annual maximum SWE.

predict a strong decrease in the snow pack over the 21st century resulting in less water available for runoff (Fig. 8). This reduction in snow pack is primarily due to increases in winter temperatures that result in less snow accumulation and increased evaporation. The correlation between winter precipitation (December–January) and maximum snow pack ($R = +0.345$) is much lower than the correlation between winter temperature (December–January) and maximum snow pack ($R = -0.800$).

Figure 9 shows the mean daily stream flow predictions for the A2 scenario for all seven GCMs for the last 30 years of the 21st century. The 1961–1990 hydrograph exhibits two distinct peaks. The first is associated with snowmelt in the lowlands and
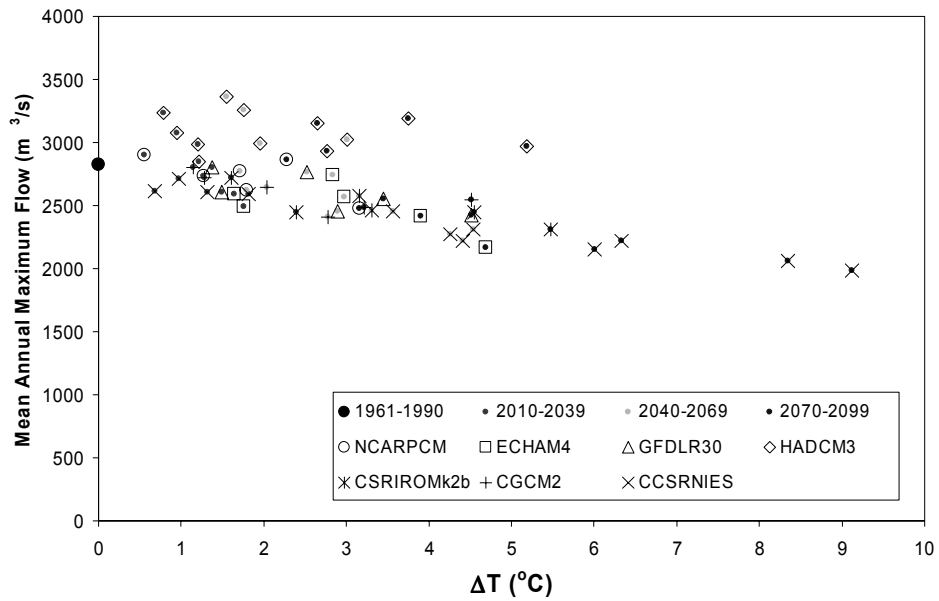
Fig. 8 Changes in mean annual maximum flow with changes in temperature.
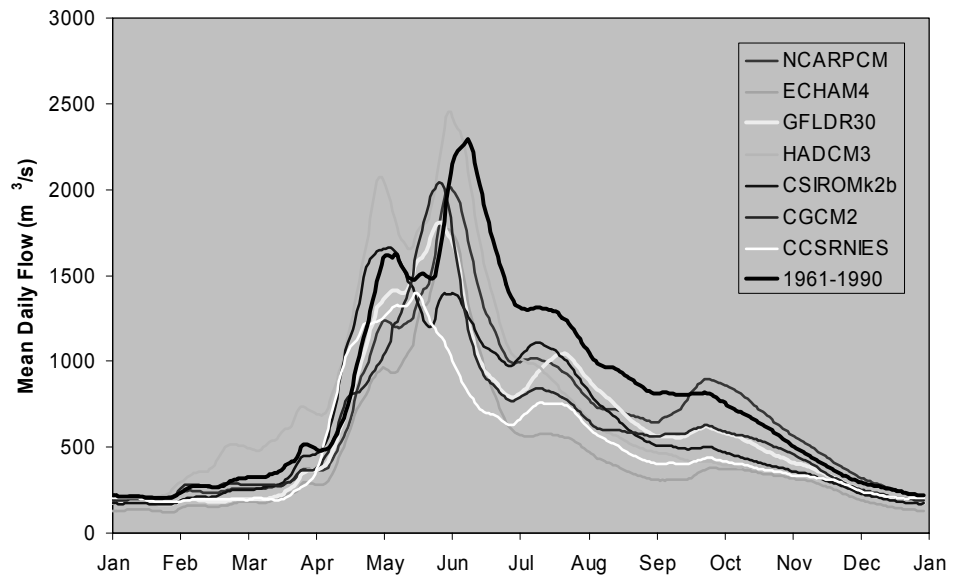

Fig. 9 Mean daily flow rates for 2070–2099 for A2 climate scenarios and observed flow rates for 1961–1990.

the second is associated with snowmelt in the mountainous southwest. The primary effect of climate change is a shrinking mountain snowmelt peak that occurs approximately two weeks earlier than in the 1961–1990 period. In the extreme case of the CCNRIES scenario, the mountain snowmelt peak virtually disappears. All seven GCMs predict significantly lower stream flows from June to November.

Given that among the GCMs' results, CGCM2's are representative of an average simulation for ARB, we further examined the mean daily streamflow for all the CGCM2 scenarios (Fig. 10). Both scenarios depict very similar patterns. Streamflows become progressively smaller as the century progresses. The lowland snowmelt event
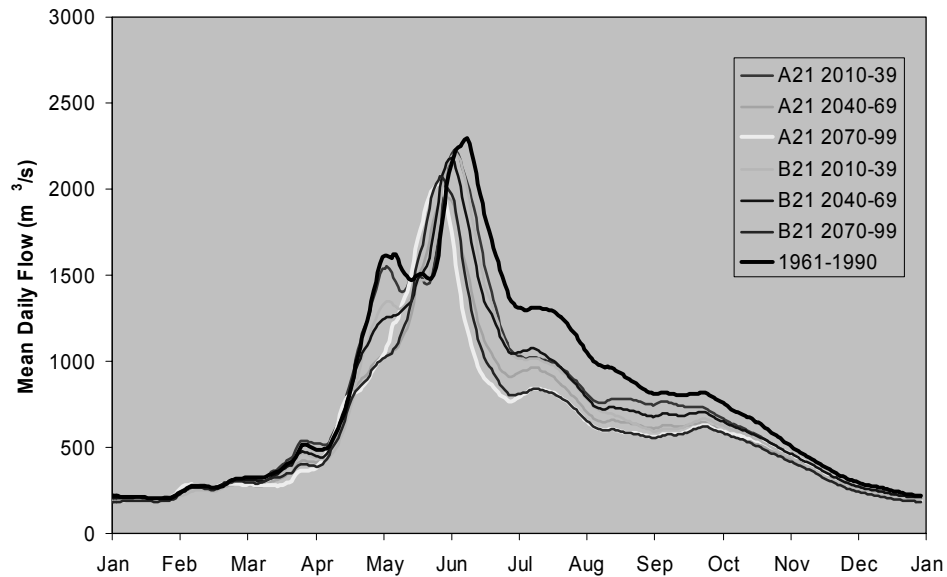
Fig. 10 Mean daily flow rates for CGCM2 climate scenarios and observed flow rates for 1961–1990.

Table 2 Changes in flow statistics for Athabasca River basin from 2070–2099 with respect to 1961–1990.

Model	Scenario	% change mean annual flow	% change max annual flow	% change min annual flow
NCAR	A21	−13.6	−14.3	8.3
	B21	−4.5	−3.2	12.6
ECHAM4	A21	−42.8	−23.8	−35.2
	B21	−35.3	−18.0	−25.1
GFDCR30	A21	−22.9	−16.2	−14.0
	B21	−25.6	−13.0	−14.9
HADCM4	A1F1	−12.4	1.2	1.0
	A21	−7.9	6.9	−8.1
	B11	−7.1	2.1	−2.6
	B21	−4.4	10.0	0.5
CSIROMk2b	A21	−21.9	−21.1	−7.1
	B21	−21.5	−20.1	−5.5
CGCM2	A21	−24.2	−15.1	0.3
	B21	−24.1	−13.6	−3.3
CCSRNIES	A1F1	−36.6	−33.6	−4.9
	A21	−36.4	−32.3	−5.4
	B21	−27.7	−27.0	−6.1
	B11	−32.7	−28.4	−9.9
Average		−22.3	−14.4	−6.6

becomes weaker and the mountain snowmelt comes earlier until the two-peak behaviour disappears. In both cases mean annual flows are predicted to decrease by almost 25% by the last third of the century. The high flow season also becomes much shorter. Historically, in an average year streamflows could be expected to stay over

1000 m^3 s^{-1} for nearly five months from late April until mid-August. For both climate scenarios, the CGCM2 predict a high flow season that lasts less than two months from early May to mid-June.

Between increasing temperature (ΔT) and mean maximum annual flow, with the exception of the HadCM3 GCM, all the models predict significant decreases in mean annual flow peaks with rising temperatures (Fig. 8). This is mainly due to the decrease in the volume of spring runoff caused by a decreased snow pack.

In terms of mean annual flow by the end of the 21st century, the ECHAM4 A21 scenario predicted the largest decrease at –42.8%, while HadCM4 B21 predicted the smallest decrease at –4.4% (Table 2). The average change in annual flow by 2070–2099 was –22.4%. The HadCM3 and NCARPCM models consistently predicted the highest flow rates, while the ECHAM4 and CCSRNIES models predicted the lowest. In terms of mean annual maximum flow, the CCSRNIES A1FI scenario predicted the largest decrease at –33.6%, while HadCM4 B21 predicted the largest increase at +10.0%. The average change in annual maximum flow by 2070–2099 was –14.4%. In terms of mean annual minimum flow, the climate scenarios usually predicted changes ranging from –10 to +10%, with –6.6% as the average predicted change.

SUMMARY AND CONCLUSIONS

After modifying the sub-grid runoff algorithm of ISBA (Interactions Soil–Biosphere–Atmosphere) by assuming the sub-grid distribution of soil moisture follows the Xinanjiang distribution, MISBA simulated accurate runoff and snow water equivalent for the Athabasca River basin (ARB) using archived forecasts from the Global Environmental Multiscale Model (GEM), and ERA-40 data of ECMWF. Simulations using the mesoscale resolution GEM data showed that these modifications significantly improved model performance. Simulations using the GCM-scale, ERA-40 re-analysis data showed that it was possible to reproduce the observed streamflow in ARB without using downscaling methods. However, a simple statistical downscaling algorithm based on the high resolution GEM data on ERA-40 data further improve the simulated streamflow of ARB. The predicted changes to mean monthly temperature and precipitation from seven GCMs for four SRES climate scenarios over the 1961–1990 base period were used to adjust the ERA-40 temperature and precipitation for ARB, over three 30-year time periods (2010–2039, 2040–2069, 2070–2100) (a total of 54 simulations). Most of the models predict continuing decreases in average, maximum, and minimum flows over the next 100 years.

REFERENCES

Cunge, J. A. (1969) On the subject of a flood propagation computation method (Muskingum Method). *J. Hydraul. Res.* **7**(2), 205–230.

Entekhabi, D. & Eagleson, P. S. (1989) Land surface hydrology parameterization for atmospheric models including subgrid scale spatial variability. *J. Climate* **2**, 816–831.

Habets, F., Noilhan, J., Golaz, C., Goutorbe, J. P., Lacarrère, P., Leblois, E., Ledoux, E., Martin, E., Ottlé, C. & Vidal-Madjar, D. (1999) The ISBA surface scheme in a macroscale hydrological model applied to the Hapex-Mobilhy area. Part 1: Model and database. *J. Hydrol.* **217**, 75–96.

Kerkhoven, E. & Gan, T. Y. (2004) A modified ISBA surface scheme for modeling the hydrology of Athabasca River basin with GCM-scale data. *Adv. Water Resour.* (submitted).

Masson, V., Champeaux, J.-L., Chauvin, F., Meriguet, C. & Lacaze, R. (2003) A global database of land surface parameters at 1-km resolution in meteorological and climate models. *J. Climate* **16**, 1261–1282.

Noilhan, J. & Planton, S. (1989) A simple parameterization of land surface processes for meteorological models. *Monthly Weather Rev.* **117**, 536–549.

Ponce, V. M. & Yevjevich, V. (1978) Muskingum-Cunge method with variable parameters. *J. Hydraul. Div. ASCE* **104**, 1663–1667.

Smith, R. E. (1983) Approximate soil water movement by kinematic characteristics. *Soil Sci. Soc. Am. Proc.* **47**, 3–8.